


Correlations of network trajectories

Lucas Lacasa^{1,*}, Jorge P. Rodríguez^{2,†} and Victor M. Eguiluz^{1,‡}¹*Institute for Cross-Disciplinary Physics and Complex Systems IFISC (CSIC-UIB), Palma de Mallorca, Spain*²*Instituto Mediterraneo de Estudios Avanzados IMEDEA (CSIC-UIB), 07190 Esporles, Spain* (Received 31 January 2022; revised 29 June 2022; accepted 23 August 2022; published 14 October 2022)

Temporal networks model how the interaction between elements in a complex system evolves over time. Just as complex systems display collective dynamics, here we interpret temporal networks as trajectories performing a collective motion in graph space, following a latent graph dynamical system. Under this paradigm, we propose a way to measure how the network pulsates and collectively fluctuates over time and space. To this aim, we extend the notion of linear correlation functions to the case of sequences of network snapshots, i.e., a network trajectory. We construct stochastic and deterministic graph dynamical systems and show that the emergent collective correlations are well captured by simple measures, and we illustrate how these patterns are revealed in empirical networks arising in different domains.

DOI: [10.1103/PhysRevResearch.4.L042008](https://doi.org/10.1103/PhysRevResearch.4.L042008)

I. INTRODUCTION

Temporal networks [1–3] are a mathematically handy way of modeling how different elements in a complex system interact and how such interactions evolve over time. While a substantial amount of research activity has studied how dynamical processes running *on* a network—e.g., diffusion, synchronization, epidemics, etc.—are affected when such a network backbone is itself dynamically modified [4–11], the program of studying the network’s intrinsic dynamics—the dynamics *of* the network—has been seldom explored [12–15], even if such intrinsic dynamics is itself indicative of the interaction dynamics taking place in complex systems.

Our contention is that, just as complex systems display collective dynamics, temporal networks perform a collective motion in a (high dimensional) phase space—a graph phase space—rather than being just an aggregation of independently varying links. Accordingly, we propose to interpret temporal networks as whole yet not punctual objects performing a trajectory in graph space governed by a latent graph dynamical system [16]. Depending on the level of description and the system under study, the dynamical rules by which the graph object evolves over time might be driven by a system’s Hamiltonian, by an effective (possibly dissipative) theory, or by stochastic processes. This perspective opens up room to describe how networks collectively pulsate and fluctuate using the solid grounding offered by dynamical systems theory and stochastic processes and time series analysis.

Here, we illustrate such a program by investigating the extension of correlation functions—classically defined to study linear autocorrelation and cross correlation of signals—to the case where the object under analysis is a network whose dynamics displays normal modes and develops linear correlations accordingly. Formally, let $\mathcal{G} = \{G(s)\}_{s=1}^N$ be an ordered sequence of N network snapshots. The index s can be associated with time t (hence addressing temporal autocorrelations), space x (i.e., spatial correlations), or some other property that allows ordering the sequence.

For concreteness we consider labeled, unweighted networks with a fixed number of m nodes and $s \equiv t$, i.e., $\mathcal{G} = \{A(t)\}_{t=1}^N$, where $A(t) = \{A_{ij}(t)\}_{i,j=1}^m$ is the adjacency matrix of the t th network snapshot. Conceptually, the autocorrelation function of an object is the inner product of itself with itself at a later time (the lag), averaged over the dynamics. Accordingly, here we propose to define the network’s *autocorrelation matrix* $\mathcal{C}(\tau)$ at lag τ as

$$\mathcal{C}(\tau) = \frac{1}{N - \tau} \sum_{t=1}^{N-\tau} [A(t) - \mu] \cdot [A(t + \tau)^T - \mu^T], \quad (1)$$

where A^T is the transpose of matrix A and $\mu = \frac{1}{N} \sum_{t=1}^N A(t)$ is the annealed adjacency matrix of the temporal network. We then coarse-grain such matrix by projecting it using the Frobenius inner product $\langle \cdot, \cdot \rangle_F$ to obtain the scalar autocorrelation $\tilde{c}(\tau)$ as

$$\tilde{c}(\tau) = \sum_t \langle A(t), A(t + \tau) \rangle_F - \langle \mu, \mu \rangle_F = \text{tr}(\mathcal{C}(\tau)), \quad (2)$$

where $\text{tr}(\cdot)$ denotes the trace operator, i.e., $\tilde{c}(\tau)$ sums up all edge autocorrelations at lag τ . The full correlation matrix \mathcal{C} takes into account not only autocorrelations (found in the diagonal of the matrix), but also cross correlations (found in the off-diagonal terms), and is conceptually close to the comemory matrix [15]. More particularly, each off-diagonal term $\mathcal{C}_{ij}(\tau)$ ($i \neq j$) displays the cross correlation

*lucas@ifisc.uib-csic.es

†jorgeprodriguez@gmail.com

‡victor@ifisc.uib-csic.es

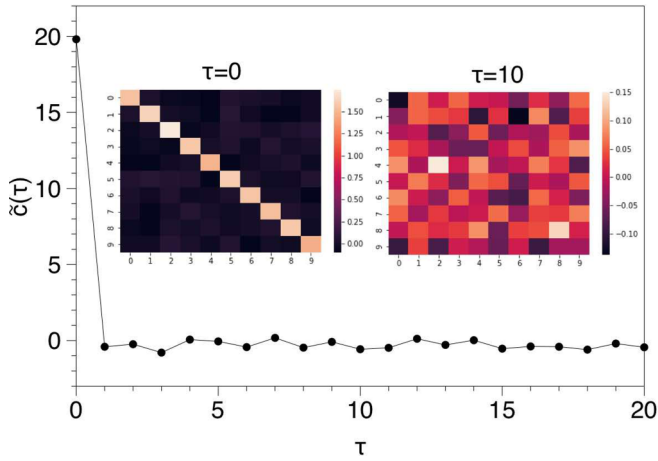


FIG. 1. White temporal networks. $\tilde{c}(\tau)$ evidences the classical Dirac-delta behavior, as expected. The insets show $\mathcal{C}_{ij}(0)$ and $\mathcal{C}_{ij}(10)$, certifying that only autocorrelations emerge, and only at the trivial $\tau = 0$.

$\sum_t A_{ik}(t)A_{jk}(t + \tau)$ of pairs of edges forming a path of size 2 between node i and node j that goes through an intermediate node k , and aggregates this over all intermediate nodes k . These off-diagonal terms aggregate the distance-2 temporal dependencies between nodes i and j that emerge as a result of their indirect correlation via the rest of the nodes, and thus provides an estimation of the network-mediated temporal dependence between nodes i and j .

II. RESULTS

To validate how $\mathcal{C}_{ij}(\tau)$ and $\tilde{c}(\tau)$ work, we proceed to create generative models of network trajectories as network extensions of benchmark dynamics.

A. White networks

An independent and identically distributed (i.i.d.) sequence of N Erdős-Rényi graphs $ER(p)$ is a network version of white noise. In Fig. 1 we show the result of $\tilde{c}(\tau)$ for $p = 0.2$,

$m = 10$, $N = 100$, showing the characteristic Dirac-delta shape of a white noise’s autocorrelation and lacking temporal cross correlations, as expected; see Supplemental Material (SM) [17].

B. Noisy periodic networks

In a second step, we build periodic networks of period T , by first constructing an i.i.d. sequence of T Erdős-Rényi graphs $ER(p)$ and then concatenating several of these sequences one after the other to build the temporal network with N snapshots. To make the quantification of periodicity more challenging, we pollute the (pure) periodic temporal network pattern with a certain amount of noise: Each edge is independently affected by noise with probability q , and those edges affected by noise are set to 1 with probability p and to 0 with $1 - p$ (by construction, the periodic pattern is completely washed out for $q \rightarrow 1$). Figure 2 illustrates the result for $(m, T, N, p, q) = (10, 20, 120, 0.1, 0.4)$. The temporal network shows a clear periodic pattern at T as its autocorrelation function peaks at $\tau = T$ and successive harmonics, and there is no trace of cross correlation or autocorrelations at $\tau \neq T$, as expected [17]. In order to quantify the periodic detectability as a function of the noise level, we compute a z score of $\tilde{c}(T)$ (see SM). In the right panel of Fig. 2, we plot such a z score as a function of q , for $T = 30$. Assuming a detectability threshold of 4 (rejecting the null hypothesis of nondetectability with very large confidence), one can assert that the noisy network has a periodic backbone up to very high noise levels $q \approx 0.9$ (this property surely depends on other parameters such as the number of nodes m , the wiring probability p , etc.).

C. Memory

As a third step, we now generate synthetic models of temporal networks with prescribed memory. We first consider the so-called discrete autoregressive network model or DARN(p) [14,15], which is the network version of a discrete autoregressive process of finite order p [18]. In this model, each link evolves independently and at each time step either makes a copy of its state from its past (taking the copy from

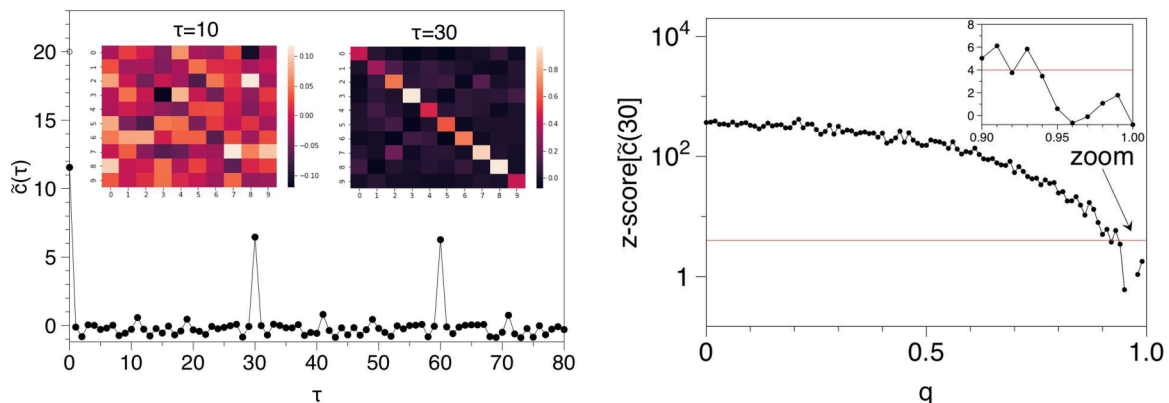


FIG. 2. Noisy periodic networks. Left: $\tilde{c}(\tau)$ evidences the peaks at multiple harmonics of the period, as expected. The insets show $\mathcal{C}_{ij}(10)$ and $\mathcal{C}_{ij}(30)$. Right: Period detectability, for which we compute the z -score statistic associated with $\tilde{c}(30)$ (see SM). As a guide, we highlight the detectability threshold z score = 4, for which the deviations between $\tilde{c}(30)$ and the average interperiod signal $\tilde{c}(1 \cdot \dots \cdot 29)$ are four times larger than expected by chance, and conclude that the hidden periodicity can be captured even for very high levels of noise.

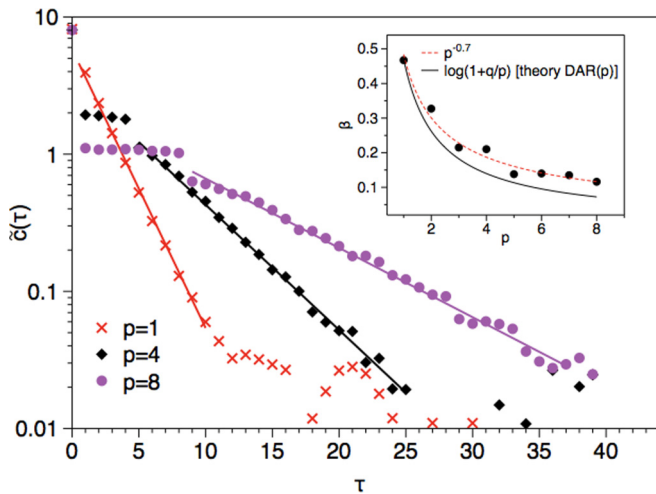


FIG. 3. DARN(p). Semilog plot of $\tilde{c}(\tau)$ for a DARN(p) of $m = 10$ nodes and $N = 10000$ snapshots, with parameters $q = 0.6$, $y = 0.1$. The network displays a constant correlation for $\tau \leq p$ and decays exponentially fast thereafter as $\exp(-\beta\tau)$. The inset describes the relation between the decaying exponent β and the order of memory p , and the best fit gives $\beta \sim p^{-0.7}$. DAR, discrete autoregressive.

a random position of its past p states) or updates randomly. Formally, the dynamics of a single link follows $l_t = Ql_{t-Z} + (1 - Q)Y$, where Q is either 0 or 1 (Bernoulli trial), Z is a random variable that draws values from $\{1, 2, \dots, p\}$, and Y is again a binary random variable that results from another

Bernoulli trial. This model generates binary values for each link l , and one can prove that overall the process is non-Markovian, with order p . In Fig. 3 we plot the values of $\tilde{c}(\tau)$ for different memory orders p . We observe that the correlation is constant for $\tau \leq p$ and seems to have an exponential decay thereafter, as expected. The rate of decay itself decreases when the memory order p increases, as shown in the inset (the solid curve corresponds to an analytical result on DAR(p) processes which involves a local approximation and is only valid when β is fitted in $p + 1 < \tau < 2p$ [18]). Overall, results suggest that $\tilde{c}(\tau)$ adequately captures the linear temporal correlations of the network.

To complete this example, we now relax the assumption that each edge samples its future state from its own past and allow, with a certain probability w , that such sampling is performed from the past of a different link. This induces non-negligible cross correlations, and as a result the network pulsation is more complex. In this scenario, $\tilde{c}(\tau)$ does not capture all the macroscopic temporal correlations, and one needs to consider the full correlation matrix $\tilde{\mathcal{C}}(\tau)$. We illustrate this effect in Fig. 4, where we can appreciate that, as the probability w increases, off-diagonal terms emerge and eventually take over the diagonal ones for large values of w .

D. Edge of chaos

We now proceed to construct deterministic temporal networks with complex dynamics, including chaos and fractality. To construct “chaotic networks,” we initially generate

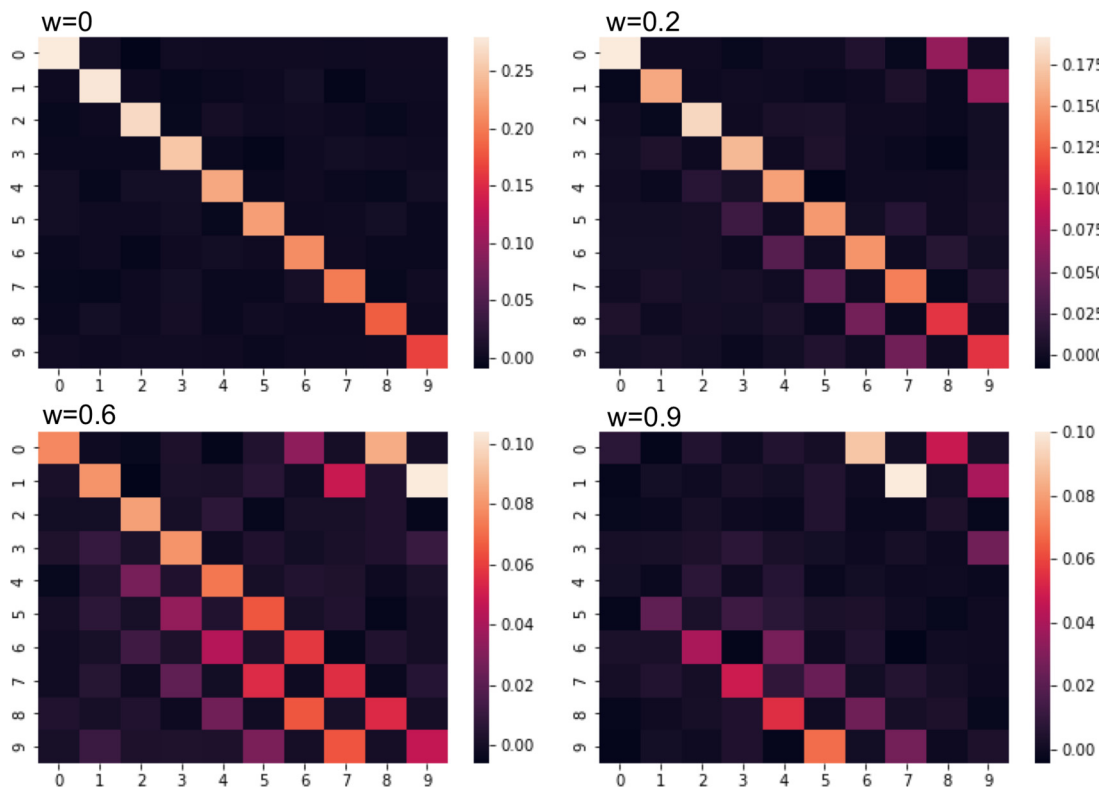


FIG. 4. Full heat-map plots of $\tilde{\mathcal{C}}_{ij}(\tau)$ for a modified DARN(1) model with $m = 10$ nodes and $N = 10^3$ snapshots, with parameters $q = 0.6$, $y = 0.1$, where with probability w , when the link update A_{ij} is from its past, we instead update it with the past of $A_{i,j'}$, $j' = j + 2 \bmod (m)$. When $w = 0$, the model is just a standard DARN(1). As w increases, the links increasingly develop network-mediated cross correlations at the expense of autocorrelations.

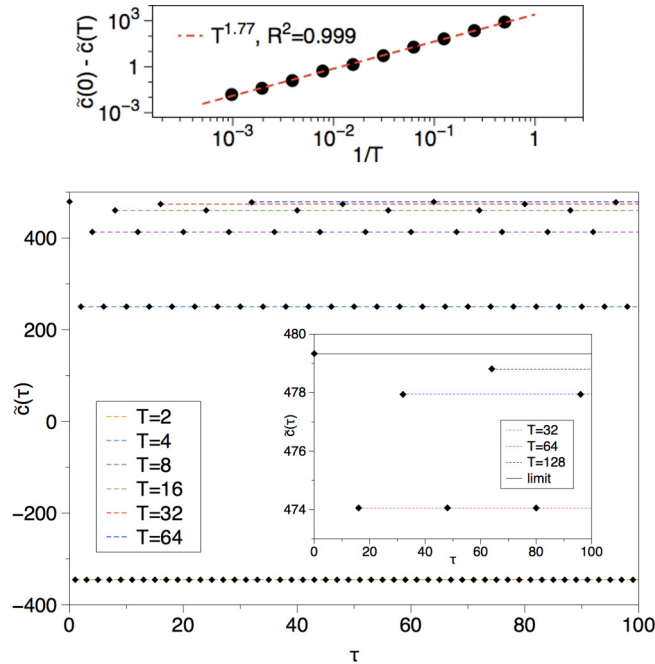


FIG. 5. Edge of chaos. Bottom: $\tilde{c}(\tau)$ for a logistic temporal network of $m = 100$ nodes and $N = 10\,000$ snapshots poised at the edge of chaos ($r \approx r_\infty$). The network trajectories display a fractal structure with infinitely many periods (hierarchically organized as powers of 2), captured as periodic peaks of different heights by the correlation function. Top: A scaling relation between such heights and the period they relate to, with a nontrivial exponent.

a dictionary of networks $\mathcal{D} = (G_1, G_2, \dots, G_L)$ such that $\|G_p - G_q\| = |p - q|$, and we “networkize” chaotic trajectories accordingly, by matching phase space points with networks from the dictionary [17]. For illustration, we choose the logistic map $x_{t+1} = rx_t(1 - x_t)$, $0 < r \leq 4$, $x \in [0, 1]$. This map generates a period-doubling cascade of signals with period $T = 2^k$ as r increases, with a period diverging at a finite $r_\infty \approx 3.569\,945\,6$. For $r > r_\infty$ the map produces chaotic trajectories intertwined with other routes to chaos.

We analyzed $\tilde{c}(\tau)$ for two interesting cases: $r = 4$ (fully developed chaos) and $r = r_\infty$ (edge of chaos), for $L = 1000$ and networks with $m = 100$ nodes and $p = 0.4$. The $r = 4$ case is indistinguishable from the case of white networks (Fig. 1), as expected given that fully developed chaos lacks linear correlations. The r_∞ case is reported in Fig. 5, finding a rich, self-similar correlation structure with an intertwined hierarchy of periodically separated peaks, reminiscent of the infinitely many modes with period $T = 2^k$ of the dynamics at the edge of chaos. The height of these peaks increases as a function of the specific mode k in such a way that, when looking at how the correlation peaks approach $\tilde{c}(0)$ (in units of the correlation function), we unveil a scaling $\tilde{c}(0) - \tilde{c}(T) \sim T^{-\alpha}$, with a nontrivial exponent $\alpha \approx 1.77$, possibly reminiscent of—although not obviously related to—Feigenbaum constants.

E. Empirical networks

To round off this study, we now apply our methodology to a range of social, technological, and biological temporal

networks that characterize evolving interaction patterns in different systems (see Appendix for details). Across these systems, we find a wide range of emerging stylized correlation patterns that match the prototypical structures found for $\tilde{c}(\tau)$ in the synthetic models, from pure periodicity—which highlights temporally pulsating networks—to both short-range and long-range correlation structures. Finer analysis of the full correlation matrices reveals the emergence of coherent groups of nodes which display network-mediated cross correlations (see Appendix). Overall, these results point to the fact that empirical temporal networks indeed describe collective fluctuations which can be captured and interpreted using our network extension of the linear correlation formalism.

III. DISCUSSION

We have presented a parsimonious way to capture the correlation structure in a sequence of networks by interpreting this sequence as a trajectory of a latent graph dynamical system. For a (complementary and) microscopic analysis of memory, we in turn refer the reader to Ref. [15]. As previously stated, the measure proposed here can equally explore temporal correlations (when the ordering index represents time) or spatial correlations, and can be trivially extended to assess cross correlations between two sequences of networks. We have certified that the trace of the correlation matrix correctly captures a range of different macroscopic temporal patterns—from periodic pulsation to decaying autocorrelations of different kinds—while the full correlation matrix is capable of finding network-mediated cross correlations between groups of links. We found that different stylized temporal correlation patterns also emerge in empirical temporal networks, which provide important insights into the collective evolution of these systems.

We foresee that applications of this method pervade physical systems, e.g., condensed matter (fluctuating spin lattices) or biophysics (proximity networks of active matter [19,20]), and include areas beyond physics such as social mobility [21], technological transportation networks, or ecological systems where spatial correlations characterize adaptation to Earth’s longitudinal or latitudinal gradients [22–25]. From a methodological viewpoint, further research should also consider the cases (i) where the vertex set size also fluctuates over time or space, (ii) where nodes do not have an explicit label, or (iii) where links are weighted or directed. Problem (i) can be tentatively addressed by sampling the maximal subgraph that contains a unique vertex set. Problem (ii) is more computationally challenging and relates to the problem of canonically embedding an unlabeled network into a labeled one; a possible solution (computationally affordable for medium-size networks) relates to labeling nodes via Hausdorff-Gromov embeddings.

In this Research Letter, we deliberately chose an intuitive property—linear correlations—to convey our idea of interpreting temporal networks as trajectories. The broader research program extends above and beyond correlations: We envisage other dynamical properties (e.g., dynamical stability) to be similarly extended to analyze network trajectories.

PYTHON implementations of all algorithms are available [26].

ACKNOWLEDGMENTS

The authors thank Oliver Williams, Konstantin Klemm, and Juan Fernández-Gracia for insightful discussions. L.L. and V.M.E. acknowledge funding from projects DYNDEEP (EUR2021-122007), MISLAND (PID2020-114324GB-C22), and Severo Ochoa and María de Maeztu Program for Centers and Units of Excellence in R&D (MDM-2017-0711) all funded by MCIN/AEI/10.13039/501100011033. J.P.R. is supported by the Juan de la Cierva Formación program (Reference No. FJC2019-040622-I) funded by the Spanish Ministry of Science and Innovation.

APPENDIX: EMPIRICAL NETWORKS

Empirical networks include online (email networks [27]) and offline social interaction in different settings (proximity networks in a university [28], a hospital ward [29], a primary school [30], a high school [31], or interactions in a village [32]), transportation networks (New York City subway, U.S. air traffic [33]), and biological systems (a protein interaction network [34]) [17]. Values of $\tilde{c}(\tau)$ for all systems are plotted in Fig. 6. We find that social-interaction-based networks typically display linear correlations at the network size that decay with different speeds but do not show evidence

of harmonicity, suggesting that the underlying complex social system evidences different degrees of memory (see also Fig. 7, where we show how temporally correlated communities strongly emerge in these systems). This contrasts with online interactions (emails), which follow a markedly regular pattern with a collective periodicity of $T \approx 1$ day, with a second periodic mode showing up at $T \approx 1$ week. Such a periodic structure—possibly reminiscent of an underlying scheduling—is also found in origin-destination flows in both subway and air transport (daily periodicity), which on the other hand display hidden, network-mediated anticorrelations, as unveiled by the full correlation matrices (see below). More surprising is to observe that periodic modes also emerge in a biological system such as a protein interaction network: Here, we speculate that the observed periodicity is related to the typical length of a full metabolic cycle [35].

To be able to visually display the full correlation matrices of empirical temporal networks, we have proceeded to preorder nodes by aggregating the adjacency matrices over all snapshots and by feeding this weighted matrix to Louvain's community detection algorithm [36]. Hence pairs of nodes whose edges have similar overall activity are initially grouped together. In Fig. 7 we have then plotted $\tilde{c}_{ij}(\tau)$ at different relevant lags. Results suggest the emergence of

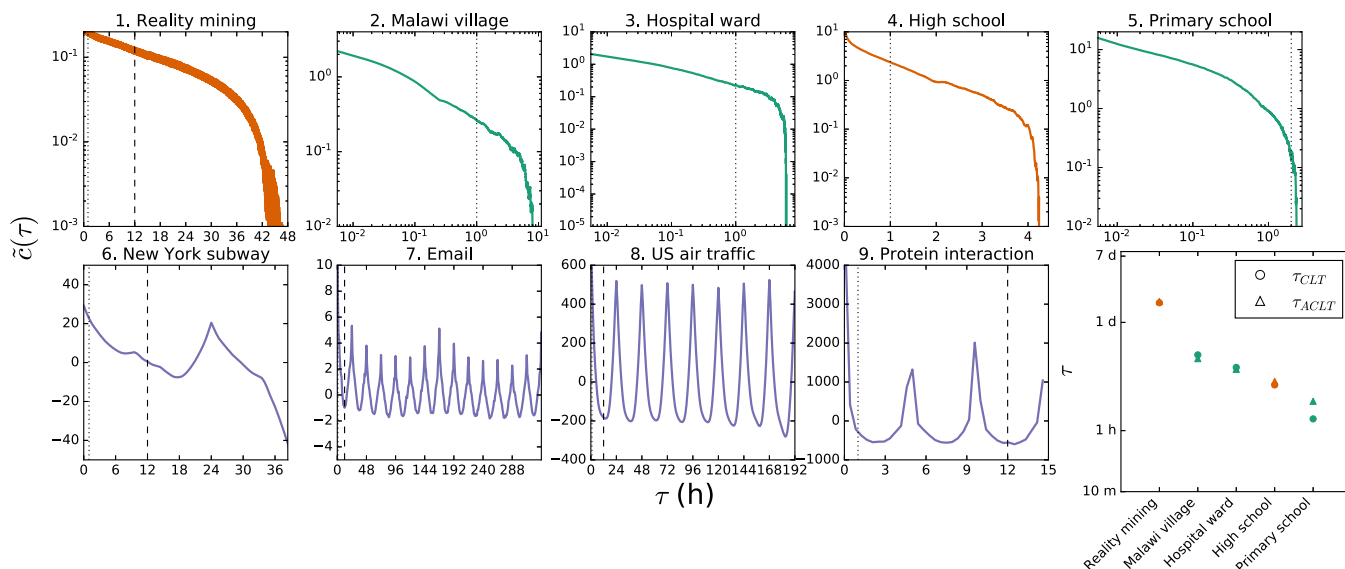


FIG. 6. Empirical networks. Plots of $\tilde{c}(\tau)$ as a function of τ (hours) for different empirical temporal networks (see the main text and the Appendix for details). Some of the panels are in semilog scale, some of them are in log-log scale, and some of them are in linear scales. The dotted and dashed vertical lines correspond to $\tau = 1$ and 12 h, respectively. Across these systems we find a wide range of emerging stylized correlation patterns that match the prototypical structures found in the synthetic models, from pure periodicity (blue)—highlighting temporally pulsating networks—to both short-range (orange) and long-range correlation structures (green). The bottom-right panel depicts the correlation lifetime τ_{CLT} and activity-preserved correlation lifetime τ_{ACLT} , defined as the first time after which the curves hit $\tilde{c} = 0$ and the first time after which the curve crosses a properly shuffled null model, respectively (these quantities are well defined only for decaying correlation curves, not so for periodic ones). For a deeper analysis of internal correlation structure, see the full correlation matrices in Fig. 7. We find that social-interaction-based networks typically display linear correlations at the network size that decay with different speeds (exponentially or with a power-law decay) but do not show evidence of harmonicity, suggesting that the underlying complex social system evidences different degrees of memory. This contrasts with online interactions (emails), which follow a markedly regular pattern with a collective periodicity of $T \approx 1$ day, with a second periodic mode showing up at $T \approx 1$ week. Such a periodic structure—possibly reminiscent of an underlying scheduling—is also found in origin-destination flows found in both subway and air transport (daily periodicity). More surprising is to observe that periodic modes also emerge in a biological system such as a protein interaction network: Here, we speculate that the observed periodicity is related to the typical length of a full metabolic cycle of ≈ 5 h [34,35].

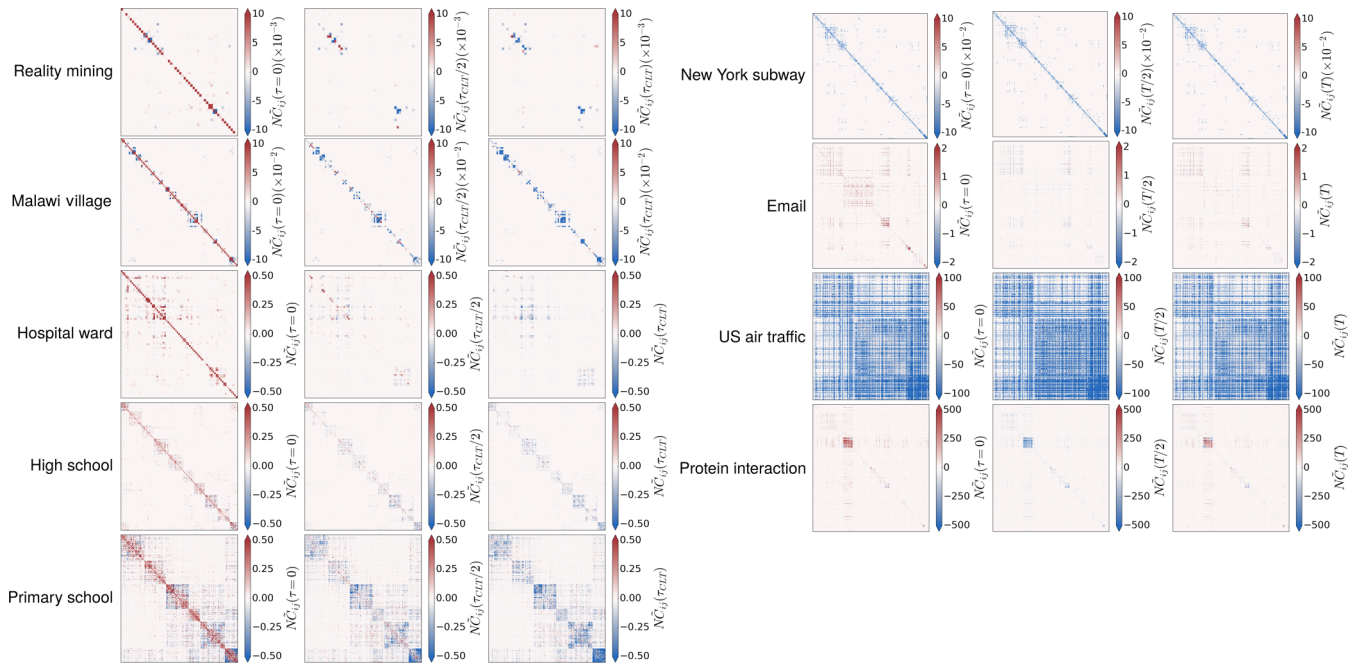


FIG. 7. Correlation matrices of empirical networks. Heat-map plots of the full correlation matrices $\tilde{\mathcal{C}}_{ij}(\tau)$ for $\tau = 0, \tau_{\text{CLT}}/2, \tau_{\text{CLT}}$ (see Fig. 6), for those empirical temporal networks where no pulsation was detected (the networks shown on the left-hand side of the figure), and for $\tau = 0, T/2, T$ for those empirical temporal networks where pulsation was previously detected in $\tilde{c}(\tau)$ at $\tau = T$ and subsequent harmonics (the networks shown on the right-hand side). The values have been multiplied by the number of nodes N so that the color code matches the scale of values found for $\tilde{c}(\tau)$. Nodes have been preordered in terms of their aggregated activity via Louvain's community detection method [36]. We can see that at lag $\tau = 0$, the reality mining network (social contacts in a university environment) only shows autocorrelations, whereas the rest of the aperiodic networks also show important network-mediated cross correlations. In pulsating networks, important network-mediated cross correlations emerge; for instance, for the U.S. air traffic activity, links are significantly anticorrelated, something reminiscent of the asynchronous nature of origin-destination flows.

network-mediated temporal cross correlations between groups of links, only visible via the preordered full correlation

matrices, that complement the macroscopic patterns captured by the trace $\tilde{c}(\tau)$.

- [1] P. Holme and J. Saramaki, Temporal networks, *Phys. Rep.* **519**, 97 (2012).
- [2] N. Masuda and R. Lambiotte, *A Guidance to Temporal Networks* (World Scientific, Singapore, 2016).
- [3] P. Holmes and J. Saramaki, *Temporal Network Theory* (Springer, New York, 2019).
- [4] N. Masuda, K. Klemm, and V. M. Eguiluz, Temporal Networks: Slowing Down Diffusion by Long Lasting Interactions, *Phys. Rev. Lett.* **111**, 188701 (2013).
- [5] J. C. Delvenne, R. Lambiotte, and L. E. C. Rocha, Diffusion on networked systems is a question of time or structure, *Nat. Commun.* **6**, 7366 (2015).
- [6] I. Scholtes, N. Wider, R. Pfitzner, A. Garas, C. J. Tessone, and F. Schweitzer, Causality-driven slow-down and speed-up of diffusion in non-Markovian temporal networks, *Nat. Commun.* **5**, 5024 (2014).
- [7] R. Lambiotte, L. Tabourier, and J.-C. Delvenne, Burstiness and spreading on temporal networks, *Eur. Phys. J. B* **86**, 320 (2013).
- [8] P. Van Mieghem and R. Van de Bovenkamp, Non-Markovian Infection Spread Dramatically Alters the Susceptible-Infected-Susceptible Epidemic Threshold in Networks, *Phys. Rev. Lett.* **110**, 108701 (2013).
- [9] T. Gross and B. Blasius, Adaptive coevolutionary networks: a review, *J. R. Soc. Interface* **5**, 259 (2008).
- [10] F. Vazquez, V. M. Eguiluz, and M. San Miguel, Generic Absorbing Transition in Coevolution Dynamics, *Phys. Rev. Lett.* **100**, 108702 (2008).
- [11] J. Ito and K. Kaneko, Spontaneous Structure Formation in a Network of Chaotic Units with Variable Connection Strengths, *Phys. Rev. Lett.* **88**, 028701 (2001).
- [12] P. Grindrod and D. J. Higham, Evolving graphs: dynamical models, inverse problems and propagation, *Proc. R. Soc. A* **466**, 753 (2010).
- [13] P. Grindrod, M. C. Parsons, D. J. Higham, and E. Estrada, Communicability across evolving networks, *Phys. Rev. E* **83**, 046120 (2011).
- [14] O. E. Williams, F. Lillo, and V. Latora, Effects of memory on spreading processes in non-Markovian temporal networks, *New J. Phys.* **21**, 043028 (2019).
- [15] O. E. Williams, L. Lacasa, A. P. Millan, and V. Latora, The shape of memory in temporal networks, *Nat. Commun.* **13**, 499 (2022).
- [16] E. Prisner, *Graph Dynamics* (Longman, Harlow, 1995).
- [17] See Supplemental Material at <http://link.aps.org/supplemental/10.1103/PhysRevResearch.4.L042008> for additional details on

- analytical derivations, algorithmic implementation, and characteristics of empirical networks.
- [18] O. E. Williams, Temporal networks and the effects of memory, Ph.D. thesis, Queen Mary University of London, 2019.
- [19] T. Sanchez, D. T. N. Chen, S. J. DeCamp, M. Heymann, and Z. Dogic, Spontaneous motion in hierarchically assembled active matter, *Nature (London)* **491**, 431 (2012).
- [20] L. Lacasa, I. P. Mariño, J. Míguez, V. Nicosia, É. Roldán, A. Lisica, S. W. Grill, and J. Gómez-Gardeñes, Multiplex Decomposition of Non-Markovian Dynamics and the Hidden Layer Reconstruction Problem, *Phys. Rev. X* **8**, 031038 (2018).
- [21] A. Stopczynski, V. Sekara, P. Sapiezynski, A. Cuttone, M. M. Madsen, J. E. Larsen, and S. Lehmann, Measuring large-scale social networks with high resolution, *PLoS ONE* **9**, e95978 (2014).
- [22] P. Descombes, T. Gaboriau, C. Albouy, C. Heine, F. Leprieur, and L. Pellissier, Linking species diversification to palaeo-environmental changes: A process-based modelling approach, *Global Ecol. Biogeogr.* **27**, 233 (2018).
- [23] R. S. Etienne, J. S. Cabral, O. Hagen, F. Hartig, A. H. Hurlbert, L. Pellissier, M. Pontarp, and D. Storch, A minimal model for the latitudinal diversity gradient suggests a dominant role for ecological limits, *Am. Nat.* **194**, E122 (2019).
- [24] P. Mannon, P. Upchurch, R. Benson, and A. Goswami, The latitudinal biodiversity gradient through deep time, *Trends Ecol. Evol.* **29**, 42 (2014).
- [25] M. Pontarp, L. Bunnefeld, J. S. Cabral, R. S. Etienne, S. A. Fritz, R. Gillespie, C. H. Graham, O. Hagen, F. Hartig, S. Huang, R. Jansson, O. Maliet, T. Münkemüller, L. Pellissier, T. F. Rangel, D. Storch, T. Wiegand, and A. H. Hurlbert, The latitudinal diversity gradient: Novel understanding through mechanistic eco-evolutionary models, *Trends Ecol. Evol.* **34**, 211 (2019).
- [26] <https://github.com/lucaslacasa/>.
- [27] R. A. Rossi and N. K. Ahmed, The Network Data Repository with interactive graph analytics and visualization, 2015, <https://networkrepository.com>.
- [28] N. Eagle and A. Pentland, Reality mining: sensing complex social systems, *Pers. Ubiquitous Comput.* **10**, 255 (2006).
- [29] P. Vanhems, A. Barrat, C. Cattuto, J.-F. Pinton, N. Khanafer, C. Régis, B.-A. Kim, B. Comte, and N. Voirin, Estimating potential infection transmission routes in hospital wards using wearable proximity sensors, *PLoS ONE* **8**, e73970 (2013).
- [30] J. Stehlé, N. Voirin, A. Barrat, C. Cattuto, L. Isella, J.-F. Pinton, M. Quaggiotto, W. Van den Broeck, C. Régis, B. Lina, and P. Vanhems, High-resolution measurements of face-to-face contact patterns in a primary school, *PLoS ONE* **6**, e23176 (2011).
- [31] R. Mastrandrea, J. Fournet, and A. Barrat, Contact patterns in a high school: a comparison between data collected using wearable sensors, contact diaries and friendship surveys, *PLoS ONE* **10**, e0136497 (2015).
- [32] L. Ozella, D. Paolotti, G. Lichand, J. P. Rodríguez, S. Haenni, J. Phuka, O. B. Leal-Neto, and C. Cattuto, Using wearable proximity sensors to characterize social contact patterns in a village of rural Malawi, *EPJ Data Sci.* **10**, 46 (2021).
- [33] M. J. Williams and M. Musolesi, Spatio-temporal networks: reachability, centrality and robustness, *R. Soc. Open Sci.* **3**, 160196 (2016).
- [34] D. Fu and J. He, DPPIN: A biological repository of dynamic protein-protein interaction network data, [arXiv:2107.02168](https://arxiv.org/abs/2107.02168).
- [35] B. P. Tu, A. Kudlicki, M. Rowicka, and S. L. McKnight, Logic of the yeast metabolic cycle: temporal compartmentalization of cellular processes, *Science* **310**, 1152 (2005).
- [36] S. Fortunato and H. Darko, Community detection in networks: A user guide, *Phys. Rep.* **659**, 1 (2016).